ALEPH 93-12
PHYSIC 93-09
P. Colas et al.
20.01.1993

A New Study of K^0 Production in Z^0 Decays

P. Colas, M.-C. Lemaire and A. Roussarie

19 Janvier 1993

Abstract

The production of K^0 mesons in e^+e^- interactions at center of mass energies in the region of the Z^0 mass has been recently investigated with the data collected by ALEPH in 1990 and 1991. It corresponds to about 453500 selected hadronic Z decays. The mean multiplicity and measured production cross-sections are compared with data obtained by the other LEP experiments and with a previous analysis of the 1990 ALEPH data.

1 Analysis method

The analysis has been carried out on approximately 453500 hadronic events collected by the ALEPH detector at LEP in 1990 and 1991 available in the nano-DST form (version 110). The choice of using nano-DST was done from speed considerations and to check if nano's are usable for Heavy Flavor decay reconstruction. The Monte Carlo sample consists of 337 K hadronic events with only the 1991 geometry. The Monte Carlo hadronic events with 1990 geometry have not been used because in that sample K_S^0 were assumed to be stable particles. The analysis has been performed by means of the informations written in the YRV0 bank by the YRMIST package[1] at the nano-DST creation. In this algorithm, the search for K_S^0 is done via their $\pi^+\pi^-$ decay products. To reduce the background contribution the following selection cuts have been applied to the K_S^0 candidates.

- the cut on the invariant mass M was applied requiring $|M - M_{K^0}|$ to be less than 40 MeV/c^2;
- a rough agreement with the mass hypothesis was set by requiring that the pull on the mass $|M - M_{K^0}|/\sigma(M)$ to be less than 5;
- a low momentum cut on the π decay tracks was set to 0.2 GeV;
- the χ^2 of the kinematic fit had to be less than 18;
- the angle θ^* between the positive decay particle and the K_S^0 direction in the K^0 center of mass system had to satisfy $|cos(\theta^*)| < 0.95$.
- the reduced proper time t/τ_{K^0} was calculated with $c\tau_{K^0}$=2.675 cm. It had to be larger than 0.25. The cut on the proper time has been chosen instead of a cut on the decay length because it follows an exponential behavior; therefore, the efficiency of such a cut is well under control. Furthermore, the proper time range where lay the background was much less momentum-dependent than for the decay length distribution.
- if a track pair gave two candidates of the same mass hypothesis but at different vertex positions, the candidate with the larger χ^2 was rejected. If two candidates shared a track, the candidate with the smallest χ^2 was kept.
- when there was a kinematic ambiguity of the K^0 candidate with $\Lambda, \bar{\Lambda}, \gamma$, the K_S^0 candidate was rejected.

In order to monitor the detection and selection efficiencies Monte Carlo data has been used. The track selection used to store their information on the nano-DST contains a cut on the distance of closest approach d_0. The tracks with $d_0 < 2$ cm were not stored; therefore, their truth association was lost. The matching had been done by requiring that the true Monte Carlo track K^{MC} is linked to the nearest reconstructed

one K^{rec} if their relative momenta and angle α satisfied the following equations:

$$\left|\frac{p_K^{rec} - p_K^{MC}}{p_K^{MC}}\right| < 0.1$$

and

$$\left|\cos\alpha(p_K^{rec}, p_K^{MC})\right| > 0.998$$

The validity of such cuts is clearly seen by comparing fig.1a and fig.1b exhibiting a scatter plot filled by either all K_S^0 candidates (fig.1a) or only those which have the two decay pions matched (fig.1b).

On fig.2 to 5 are shown comparisons between Monte Carlo and data in different momentum slices for the following various distributions:

- $\cos\theta^*$: the π^+ decay angle in the K_S^0 center of mass system. The effect of the low momentum cut on the decay track and the removal of Λ ambiguities are clearly seen on fig.2a and fig.2b;
- φ_R: the rotation angle of the decay plane with respect to the production plane;
- $|M - M_{K^0}|$: the difference between the $\pi^+\pi^-$ invariant mass and the K^0 mass;
- t/τ_{K^0}: the proper time; the loss of events at high proper time and high momentum is due to decays escaping the TPC outer radius. It shows that combinatorial background can be efficiently removed by the cut on the reduced proper time at 0.25.

The agreement between data and Monte Carlo distributions normalized to the same number of entries is excellent in all momentum slices.

2 Differential cross-sections

In order to extract the K^0 mean multiplicity and differential cross-section, it was necessary to estimate the amount of background under the signal and to correct for the detection efficiency and branching ratios. For this purpose, the differential cross-sections have been studied with three variables: the fractional momentum x_p (x_p=p_K/p_{beam}), the fractional energy x_E (x_E=E_K/E_{beam}) and ξ ($\xi = -\ln(x_p)$). In each case, the background was taken as the unmatched track distribution in the same bin slice as the data and the correction of detection efficiency was performed in each slice by calculating:

$$\epsilon = n^{K_s^0}_{recontructed}/n^{K_s^0}_{generated}$$

The corresponding detection efficiencies are compared with those of DELPHI[2] and OPAL[3] detectors respectively in fig.9 and fig.10. It

shows clearly that ALEPH is the most efficient detector. Its efficiency is momentum-dependent having a maximum of about 55% around 4.5 GeV/c. This leads to a global efficiency of 37% for a purity of 94.6%.

From figures 6,7,8 it is clear that the Monte Carlo does not reproduce the differential cross-sections as a function of momentum. For instance, fig.6 shows that the Monte Carlo overestimates the data for $x_p < 0.8$ while for $x_p > 0.8$ it underestimates the data. The discrepancies seen in the x_E and ξ distributions reflects the same effect: the data distributions are harder than the predicted ones.

3 Comparison with other analyses of LEP data

All the cross-sections and rates discussed in the present note have been corrected by the branching ratio $K^0_S \to \pi^+\pi^-$. Accurate comparisons with DELPHI and OPAL can only be done in ranges of restricted variables for which tables have been published. The differential cross-sections $(1/\sigma_{had})(d\sigma/dx_p)$ as a function of the fractional momentum x_p are shown in fig.11 for ALEPH present analysis and DELPHI analysis. Integrating the cross-sections on the same x_p range (0.005–0.3) leads to 1.97 ± 0.05 for DELPHI and 1.80 ± 0.01 for ALEPH, i.e. present ALEPH analysis gives a mean multiplicity 9% lower than DELPHI.

In fig.12 are compared the $(1/\sigma_{had})(d\sigma/d\xi)$ differential cross-sections from the present analysis and from OPAL. Integrating these cross-sections over the same ξ range (0.0–5.0) leads to 2.12 ± 0.05 for OPAL and 1.92 ± 0.01 for ALEPH; which is 9% lower than the OPAL value.

The differential cross-sections $(1/\sigma_{had})(d\sigma/d\xi)$ as a function of ξ from present analysis is compared in fig.13 with the results of the previous ALEPH analysis[4] of the 1990 data. The agreement is fairly good except around the maximum at $\xi = 2.5$ where the present K^0 cross-sections are slightly smaller than in the previous analysis. A summary of the different K^0 multiplicities is given in table 1. The present analysis leads to a mean multiplicity lower than all the others. On fig.14 is shown the cross-sections of the present analysis integrated from either x_p^{min} to 1 or $\xi = 0$ to $\xi^{max} = -Lnx_p^{min}$. The rates obtained from the two distributions are in good agreement with each other and the saturation observed at high ξ^{max} shows that there is no extrapolation error. Varying the t/τ cut from 0.25 to 0.5, leads to a variation of the mean multiplicity from 1.921 ± 0.013 to 1.939 ± 0.015. Similarly, by performing the analysis only on 1991 data with the 1991 Monte-Carlo results in a variation of the mean multiplicity from 1.921 ± 0.013 to 1.944 ± 0.016.

4 Systematic effects and uncertainties

The systematics have been studied in three parts : those arising from background subtraction, those from efficiency correction, and those due

Tableau 1: K^0 mean multiplicity

Analysis	K^0 **rate**
ALEPH present (no corr. of syst. effects)	$1.921 \pm 0.013_{stat}$
ALEPH draft	$2.11 \pm 0.015_{stat} \pm 0.05_{sys}$
DELPHI	$2.12 \pm 0.05_{stat} \pm 0.14_{sys}$
OPAL	$2.11 \pm 0.02_{stat} \pm 0.14_{sys}$

to the matching procedure described in section 1. Their estimated contributions (or upper limits on them) are given in table 2. The uncertainty on the combinatorial background was estimated using the events at $t/\tau < 0.15$, where it dominates. The rate of such events is overestimated by 8.5% by the Monte Carlo. Changing by 10% the predicted amount of background in momentum bins leads to an uncertainty of 8×10^{-3}. Taking at face value the 8.5% overestimation of background leads us to apply a 1.007 correction factor to the rate. This is confirmed by repeating the analysis raising the cut on $t/\tau_{K^0_S}$ from 0.25 to 0.5 to lower further the background, as mentioned above : the rate increases from 1.921 to 1.939.

The uncertainty on the background from real $V^0 s$ is found to be very small : 7×10^{-4}, assuming that this 0.33% contribution is known to better than 20%.

The efficiency is subject to systematic effects, if some of the distributions are not correctly reproduced by the Monte Carlo. On a variable-by-variable basis, one can compare the effect of the selection cuts on the Monte Carlo and on the data. The most important systematics comes from the least well reproduced distribution i.e. the χ^2 of the kinematic fit. The discrepancy can be seen from fig. 15 (the small background as predicted with the Monte Carlo has been subtracted in this figure). The Monte Carlo distribution is less spread than the data, which shows that the errors are underestimated in the Monte Carlo. Extrapolating the two distributions using a functional form (an exponential) allows one to estimate the efficiency of the $\chi^2_{Kinem.}$ cut in the data and Monte Carlo separately. Values of 0.91135 and 0.93939 are found respectively. We correct for this discrepancy by applying a correction factor of 1.0307 to the rate, and, conservatively, we assess the uncertainty to be at the same level : $\pm 3\%$. A more detailed study of the reasons of the discrepancy on the χ^2 distribution would need further studies.

A large source of inefficiency is the requirement of at least 4 TPC hits. Fig. 16 shows this distribution for data and Monte Carlo. One notes a shift of the average number of hits by 0.3, showing some hit reconstruction or association inefficiency in the data, not taken into ac-

count in the Monte Carlo. A shift of ± 0.3 hit of the distribution would reflect as a change of $\pm 4 \times 10^{-3}$ on the efficiency. We apply a correction factor of 1.004 and take this as an uncertainty.

For the other cuts, the data distribution is in very good agreement with the Monte Carlo, and the difference of loss due to this cut between Monte Carlo and data has been taken as a conservative estimate of the uncertainty.

We also questioned the matching procedure itself. On the basis of figures 1a and 1b, one can estimate the matching inefficiency and the background of fake matching. They have a very small effect on the data.

Correcting for the above-mentioned effects and adding the various sytematic errors in quadrature leads to the measurement :

$$N_{K^0} \; per \; hadronic \; event = 2.002 \pm 0.013(stat) \pm 0.064(syst)$$

Tableau 2: Systematic errors

Source	**relative contribution** ($\times 10^{-4}$)
Backgrounds	
Combinatorial	80
Λ	7
K^0_L	negl.
Efficiency	
t/τ	negl.
$\cos\theta^*$	0
$M_{\pi\pi}$	negl.
pull on mass	8
elim. of doubles	50
elim. of Λ's	35
p(tracks) > 0.2	negl.
$\chi^2_{GEOM} < 18$	300
$N_{hits}(TPC) \geq 4$	40
matching procedure	
matching effic.	4
fake matchings	2

5 Proper time distribution

The K^0 proper time distribution exhibited in fig.17 has been obtained from the data after background subtraction and correction for detection

efficiency. The solid line corresponds to a χ^2 fit to an exponential function for the proper time range [0.4–5.]. It leads to a K^0 lifetime in good agreement with the world average as $\tau_{K^0} = (0.8864 \pm 0.0051) 10^{-10} s$ which can be compared to the P.D.G. value:$\tau_{K^0} = (0.8922 \pm 0.0020) 10^{-10} s$.

6 Conclusion

The differential and total cross-sections for K^0 production have been measured from 453500 hadronic decays of Z recorded with the ALEPH detector in 1990 and 1991. The average efficiency is quite high(37%) for a purity of 94.6%. The detection and selection efficiency are about twice larger than OPAL and DELPHI corresponding numbers. All distributions were in very good agreement with the Monte Carlo, except those where the momentum distribution comes into play and those related to the kinematic fit. Including corrections for these systematic effects, the multiplicity per event found in the present analysis is $2.002 \pm 0.013 \pm 0.064$, which tends to be lower than the values obtained previously from 1990 data by ALEPH, OPAL and DELPHI. The measured K^0_S lifetime agrees very well with the PDG value. A reduction of the systematic uncertainty would require a better understanding of the χ^2 distribution of the kinematical fit and a direct estimate of the background. The present accuracy is however sufficient for most of the charm decay studies.

References

1) B. Rensch; ALEPH-note 90-108

2) DELPHI Collaboration; Phys. Lett. B275(1992)231

3) OPAL Collaboration; Phys.Lett. B264(1991)467

4) B. Rensch et al.; draft 1.0 of the paper,'K^0 and Λ Production in Hadronic Decays of the Z'

File: [LEMAIRE]DS5MC.HIS;1

ID	IDB	Symb	Date/Time	Area	Mean	R.M.S.
2005	1	-2	921125/1712	6.2842E+04	0.9999	3.6588E-04
					6.1352E-03	8.4378E-03

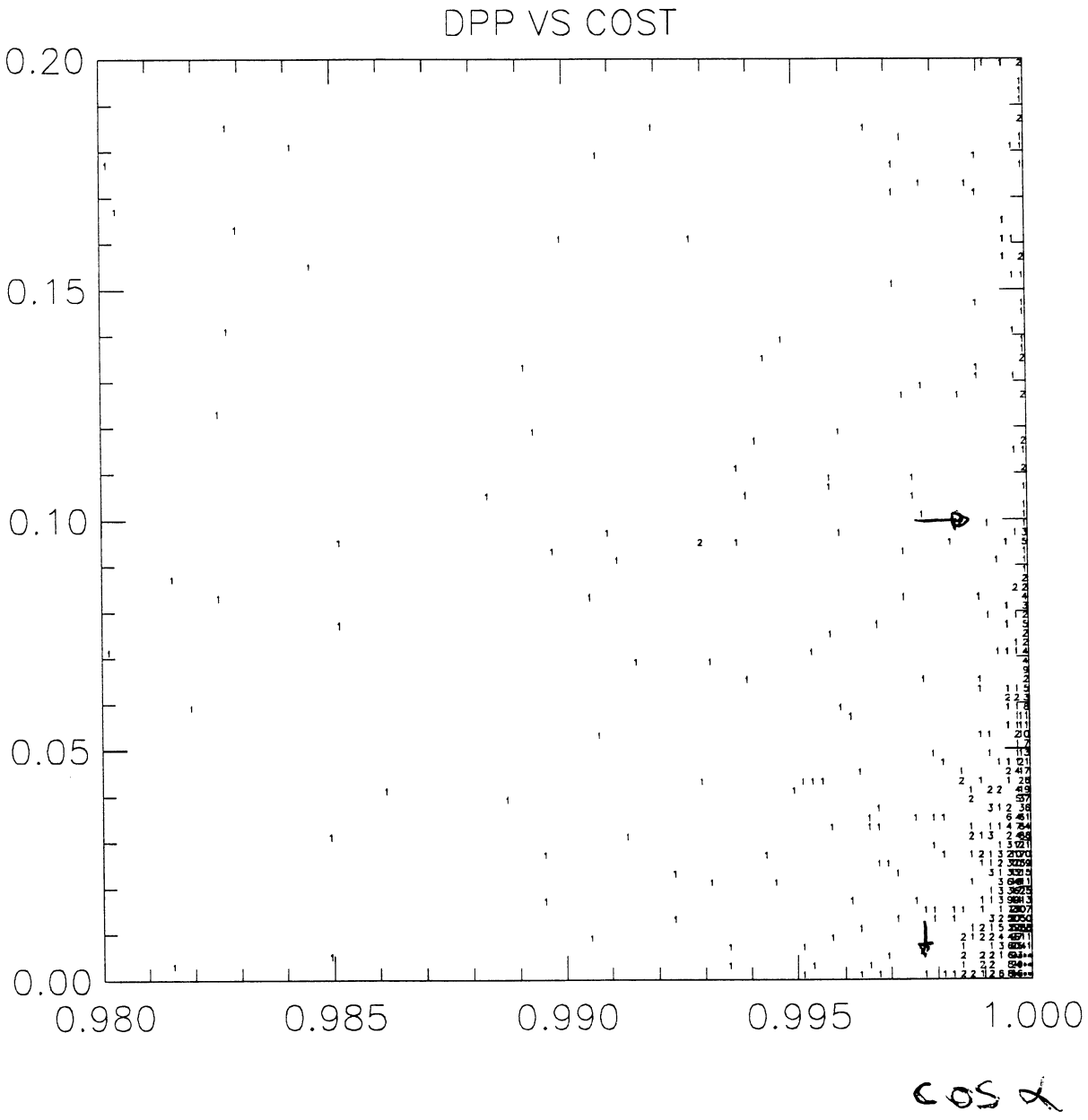

Fig. 1a

File: [LEMAIRE]DS5MC.HIS;1

ID	IDB	Symb	Date/Time	Area	Mean	R.M.S.
2006	1	-2	921125/1712	3.6957E+04	0.9999	8.2460E-05
					5.8166E-03	5.8765E-03

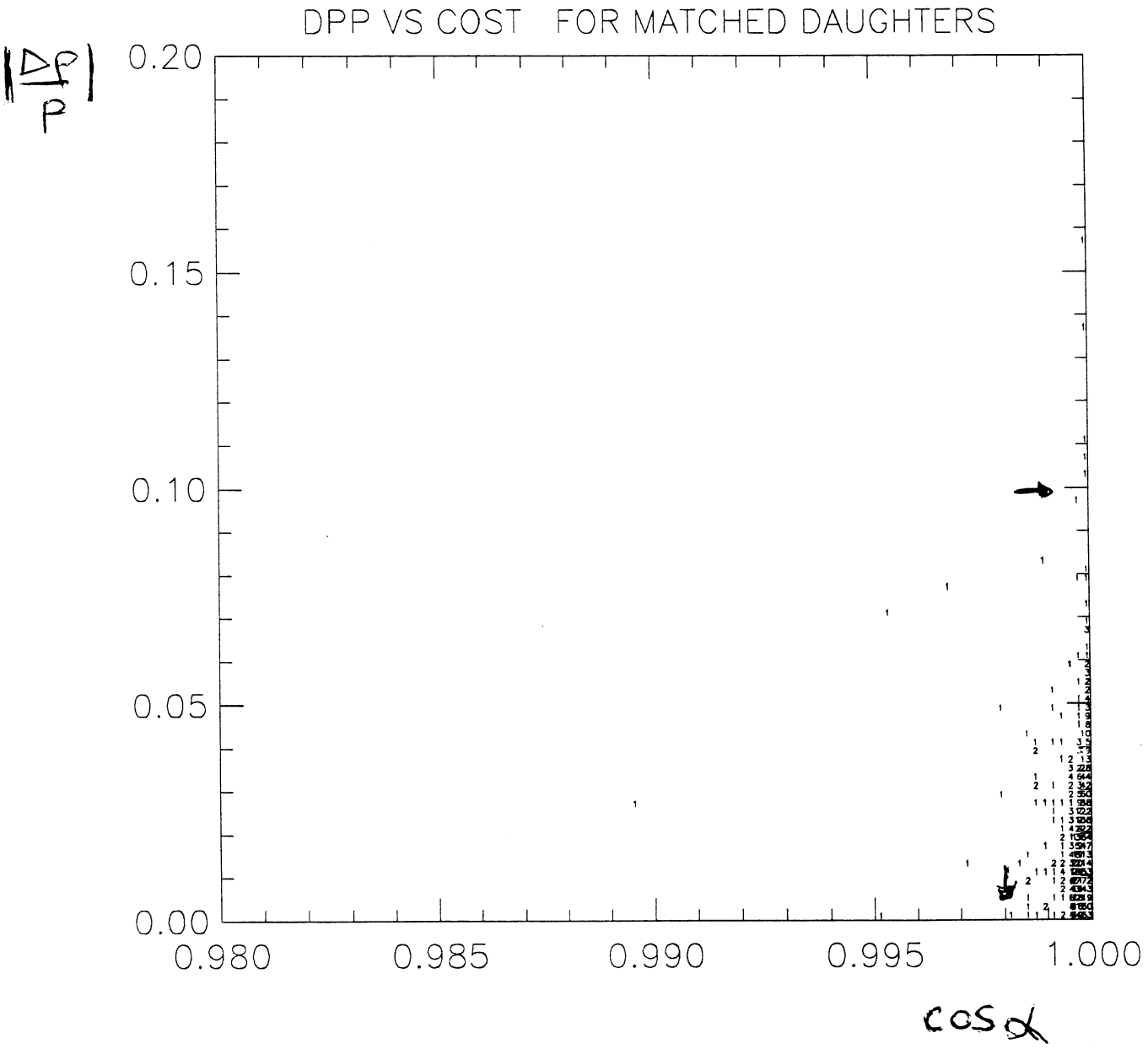

File: [LEMAIRE]DS5DT.HIS;1

ID	IDB	Symb	Date/Time	Area	Mean	R.M.S.
1302	0	-41	921123/0903	9465.	-3.7560E-03	0.3586
1302	10	1	921123/0926	9465.	4.0396E-03	0.3559
1322	0	-41	921123/0903	2.2953E+04	4.5699E-04	0.4703
1322	10	1	921123/0927	2.2953E+04	1.7181E-03	0.4699

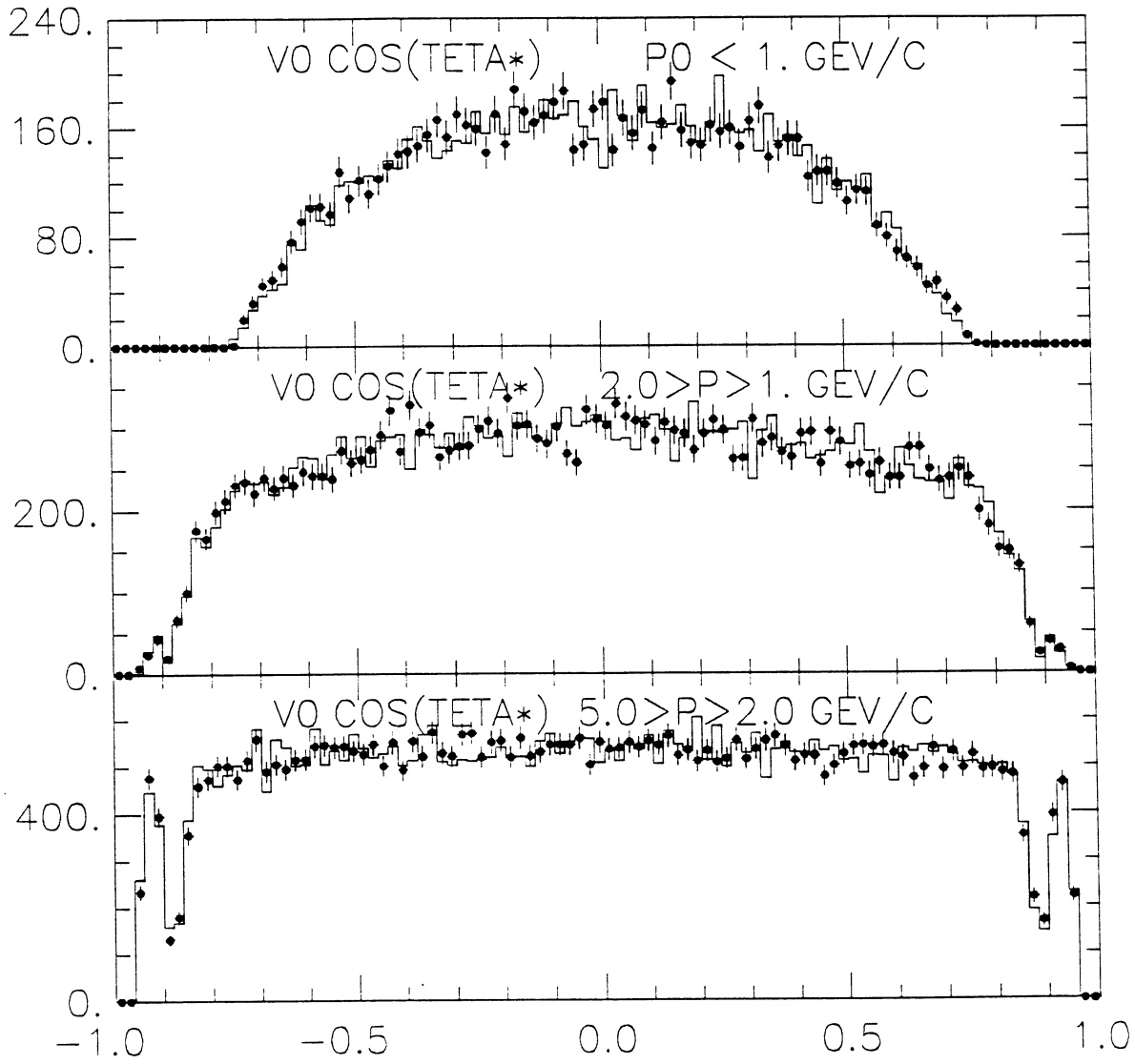

Fig. 2a

File: [LEMAIRE]DS5DT.HIS;1

ID	IDB	Symb	Date/Time	Area	Mean	R.M.S.
1362	0	-41	921123/0903	3.0567E+04	2.1556E-03	0.5188
1362	10	1	921123/0930	3.0567E+04	-1.5966E-03	0.5200
1382	0	-41	921123/0903	1.0198E+04	6.4856E-03	0.5090
1382	10	1	921123/0930	1.0198E+04	-7.3192E-03	0.5214

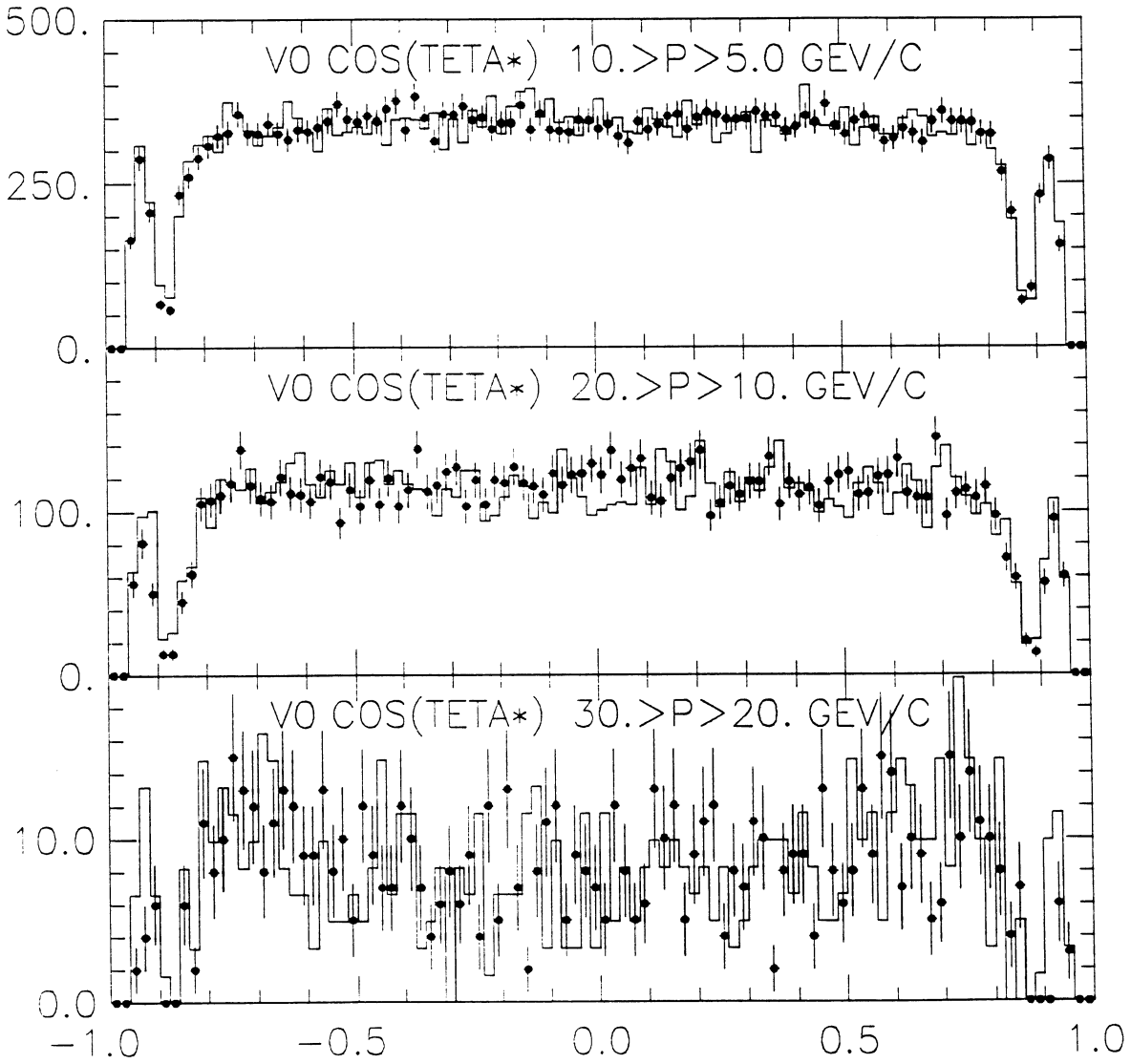

Fig. 2b

File: [LEMAIRE]DS5DT.HIS;1

ID	IDB	Symb	Date/Time	Area	Mean	R.M.S.
1303	0	-41	921123/0903	9435.	180.7	104.6
1303	10	1	921123/0939	9435.	180.6	103.5
1323	0	-41	921123/0903	2.2915E+04	180.1	103.3
1323	10	1	921123/0940	2.2915E+04	179.3	103.2

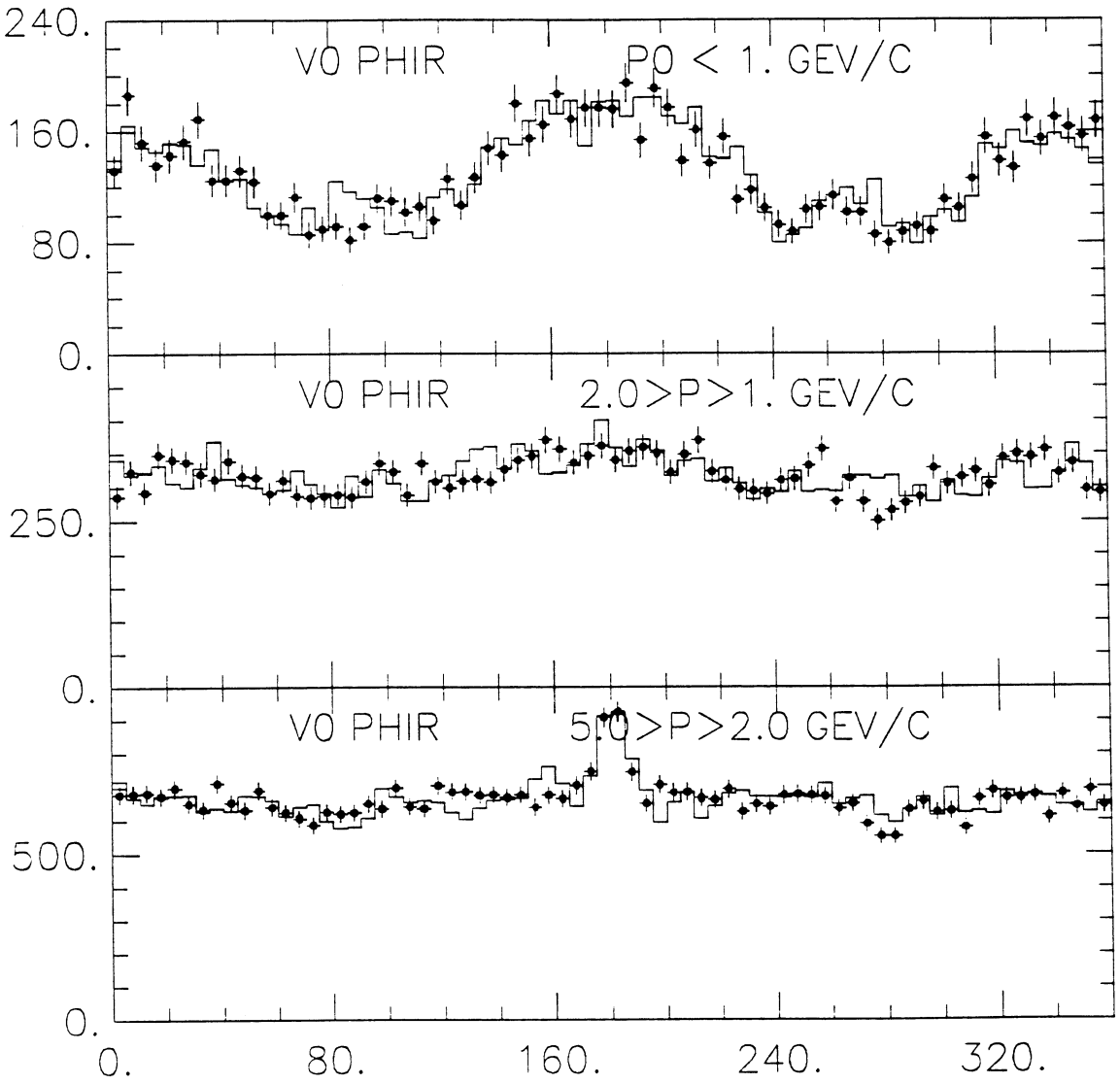

Fig. 3a

File: [LEMAIRE]DS5DT.HIS;1

ID	IDB	Symb	Date/Time	Area	Mean	R.M.S.
1363	0	-41	921123/0903	3.0505E+04	181.1	102.7
1363	10	1	921123/0942	3.0505E+04	179.8	102.4
1383	0	-41	921123/0903	1.0181E+04	178.7	93.22
1383	10	1	921123/0942	1.0181E+04	179.2	92.11

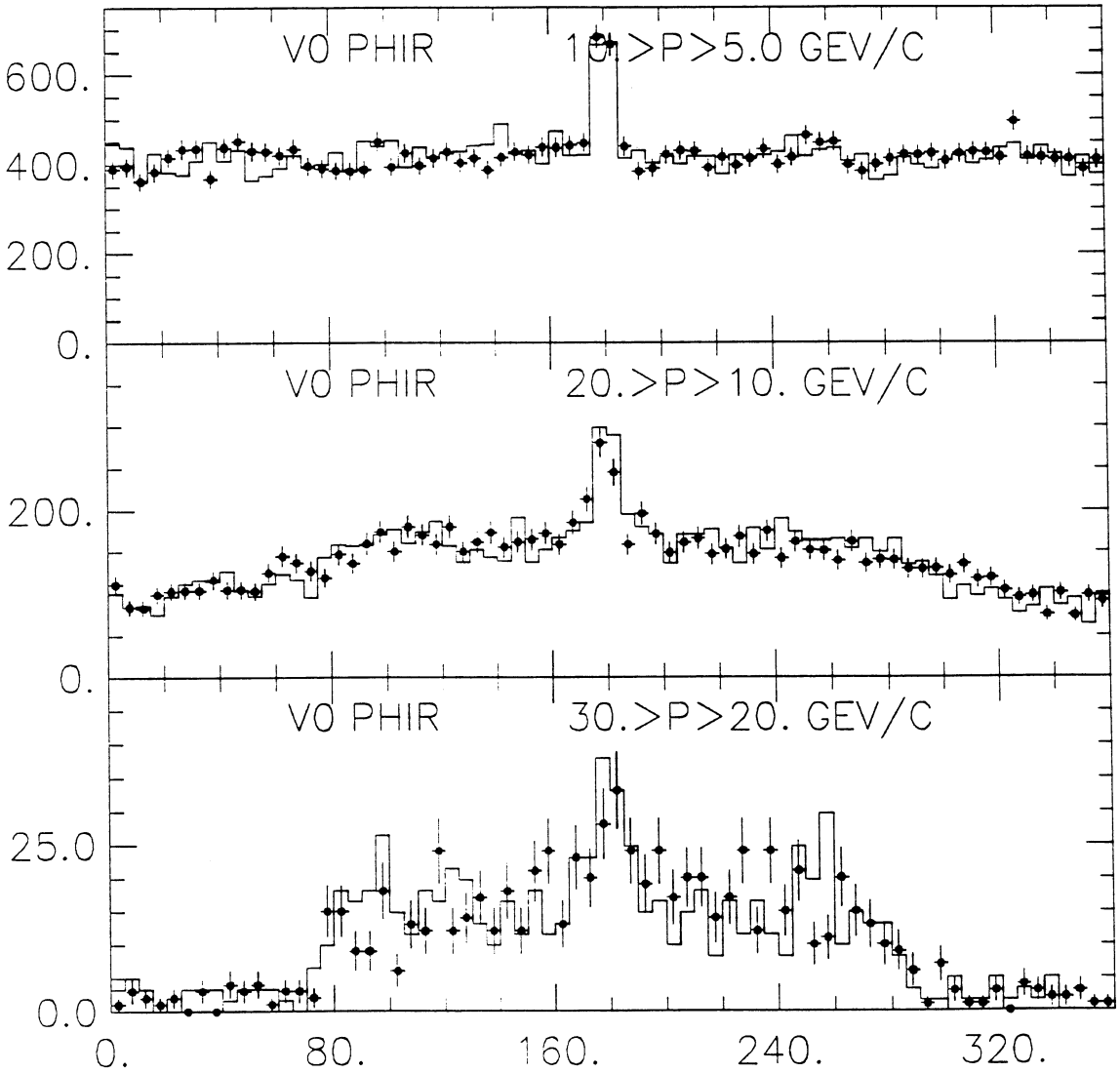

File: [LEMAIRE]DS5DT.HIS;1

ID	IDB	Symb	Date/Time	Area	Mean	R.M.S.
1306	0	-41	921123/0903	9378.	-3.018	6.112
1306	10	1	921123/0944	9378.	-3.100	5.600
1326	0	-41	921123/0903	2.2834E+04	-1.564	5.181
1326	10	1	921123/0945	2.2834E+04	-1.652	4.808

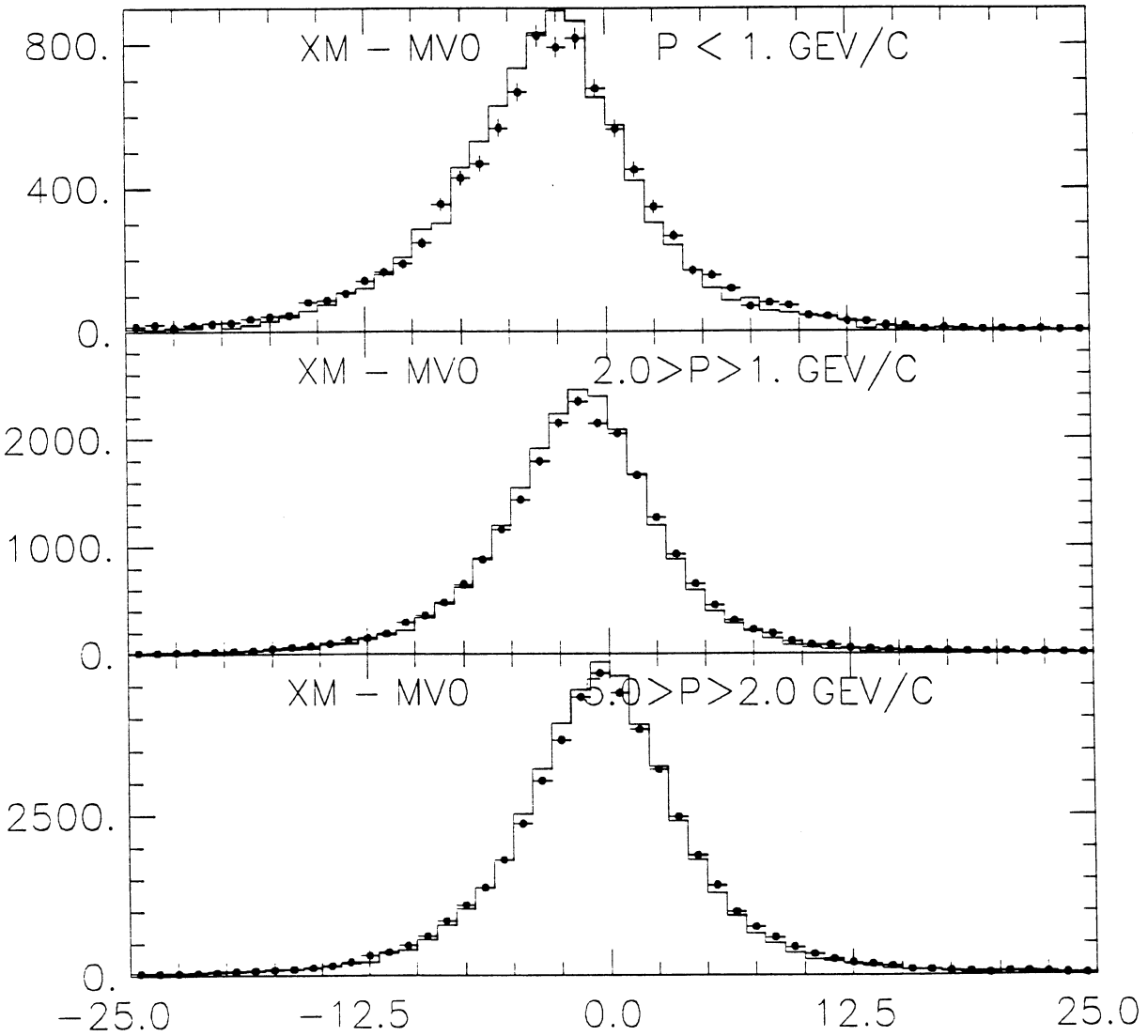

Fig 4a

File: [LEMAIRE]DS5DT.HIS;1

ID	IDB	Symb	Date/Time	Area	Mean	R.M.S.
1366	0	-41	921123/0903	2.9580E+04	0.1065	7.706
1366	10	1	921123/0947	2.9580E+04	-9.7848E-02	7.725
1386	0	-41	921123/0903	9082.	0.6885	10.85
1386	10	1	921123/0948	9082.	-9.5384E-02	10.98

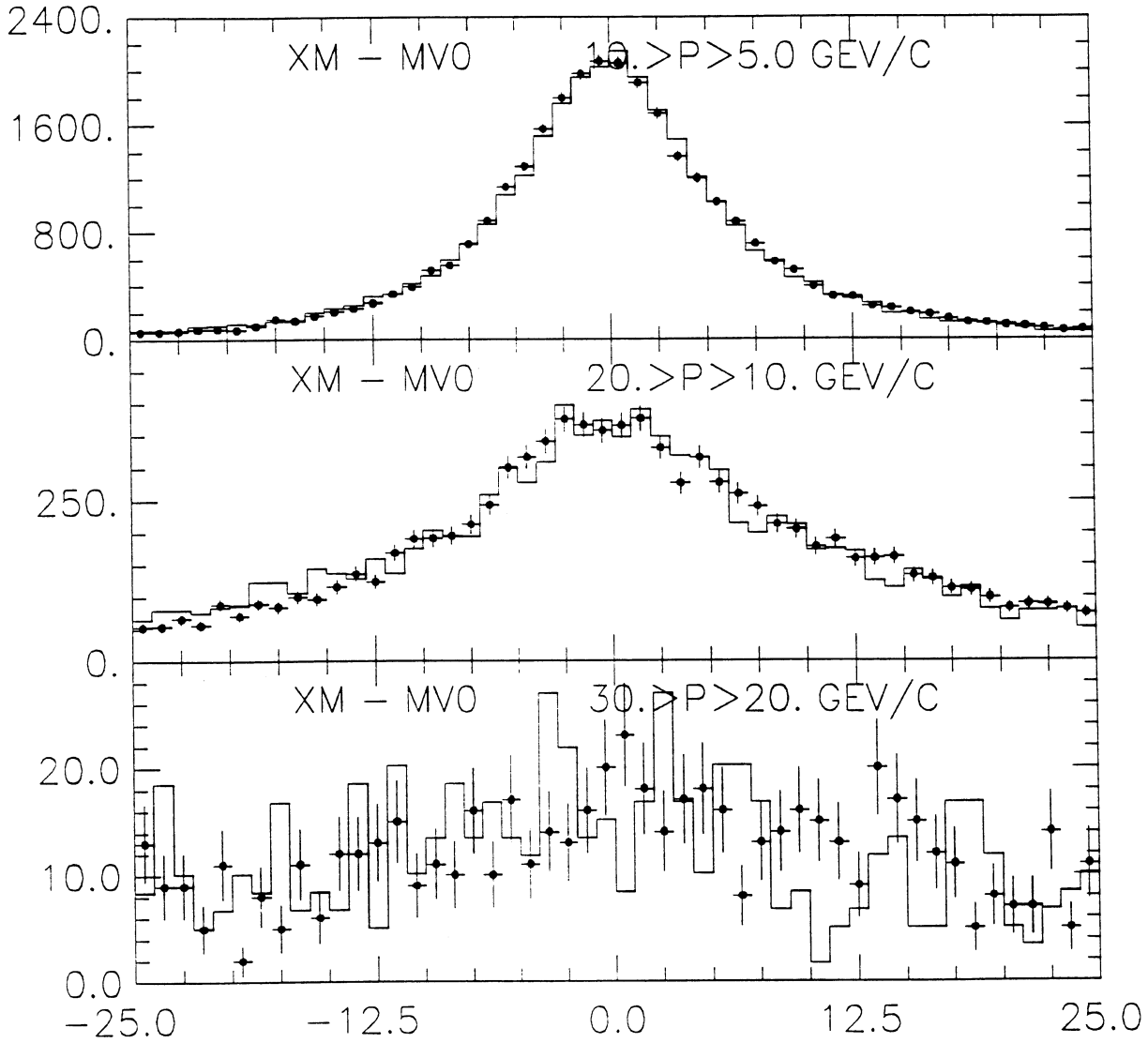

File: [LEMAIRE]DS5DT.HIS;2

ID	IDB	Symb	Date/Time	Area	Mean	R.M.S.
1305	0	-41	921123/1351	2.0550E+04	0.5776	0.8339
1305	10	1	921123/1420	2.0550E+04	0.6061	0.8515
1325	0	-41	921123/1351	4.9915E+04	0.6102	0.8626
1325	10	1	921123/1421	4.9915E+04	0.6154	0.8560

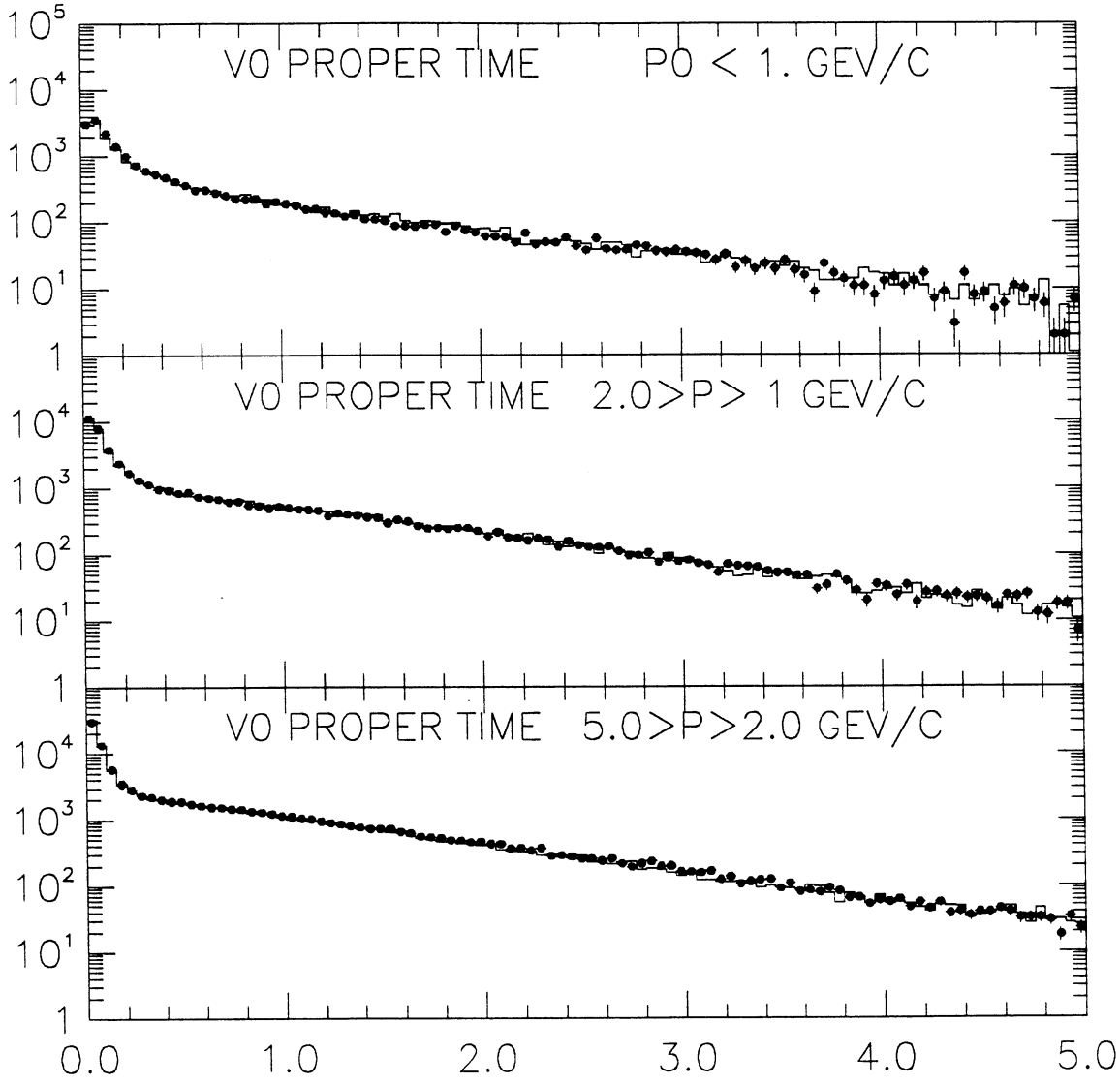

fig 5a

File: [LEMAIRE]DS5DT.HIS;2

ID	IDB	Symb	Date/Time	Area	Mean	R.M.S.
1365	0	-41	921123/1351	6.4013E+04	0.5582	0.7497
1365	10	1	921123/1423	6.4013E+04	0.5031	0.7115
1385	0	-41	921123/1351	2.5761E+04	0.3385	0.4509
1385	10	1	921123/1424	2.5761E+04	0.3085	0.4420

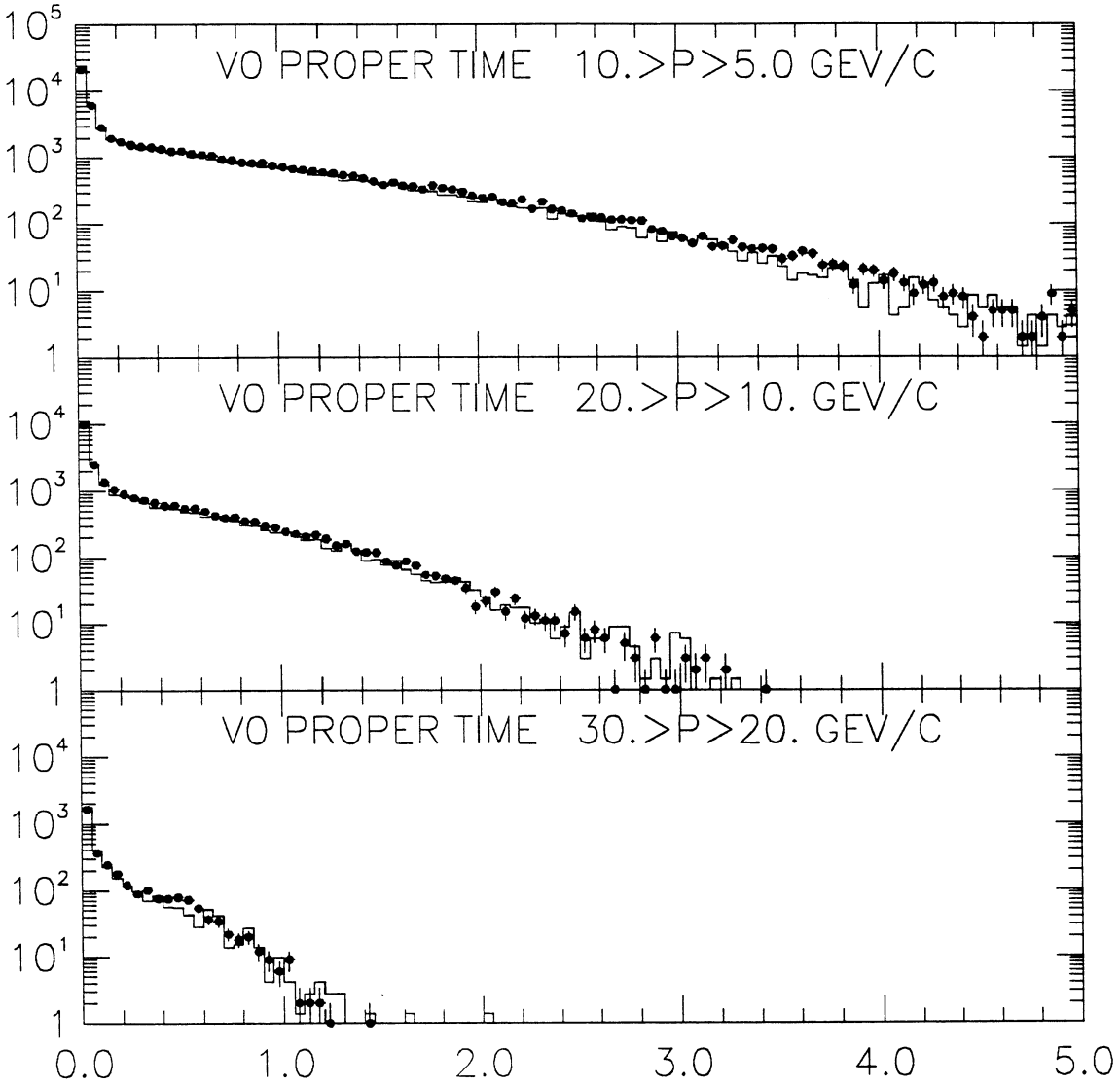

Fig 5b

File: Generated internally

ID	IDB	Symb	Date/Time	Area	Mean	R.M.S.
1444	30	-41	921119/0928	96.31	0.1079	0.1108
2016	30	1	921119/0929	100.7	9.4189E-02	0.1039

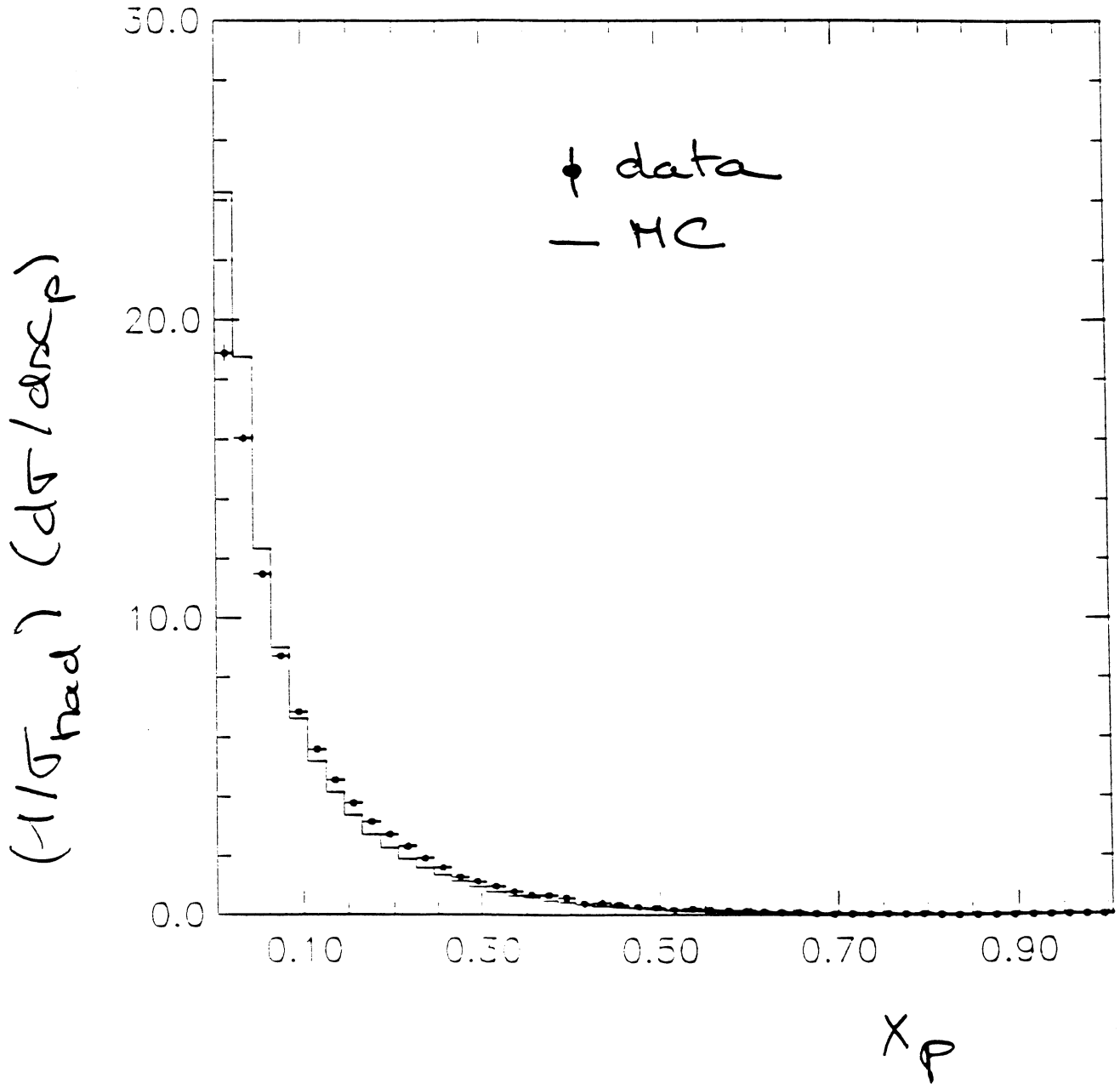

Fig. 6

File: Generated internally

ID	IDB	Symb	Date/Time	Area	Mean	R.M.S.
1442	30	-41	921120/0951	210.4	0.1022	0.1091
2011	30	1	921120/0952	226.7	8.7021E-02	0.1002

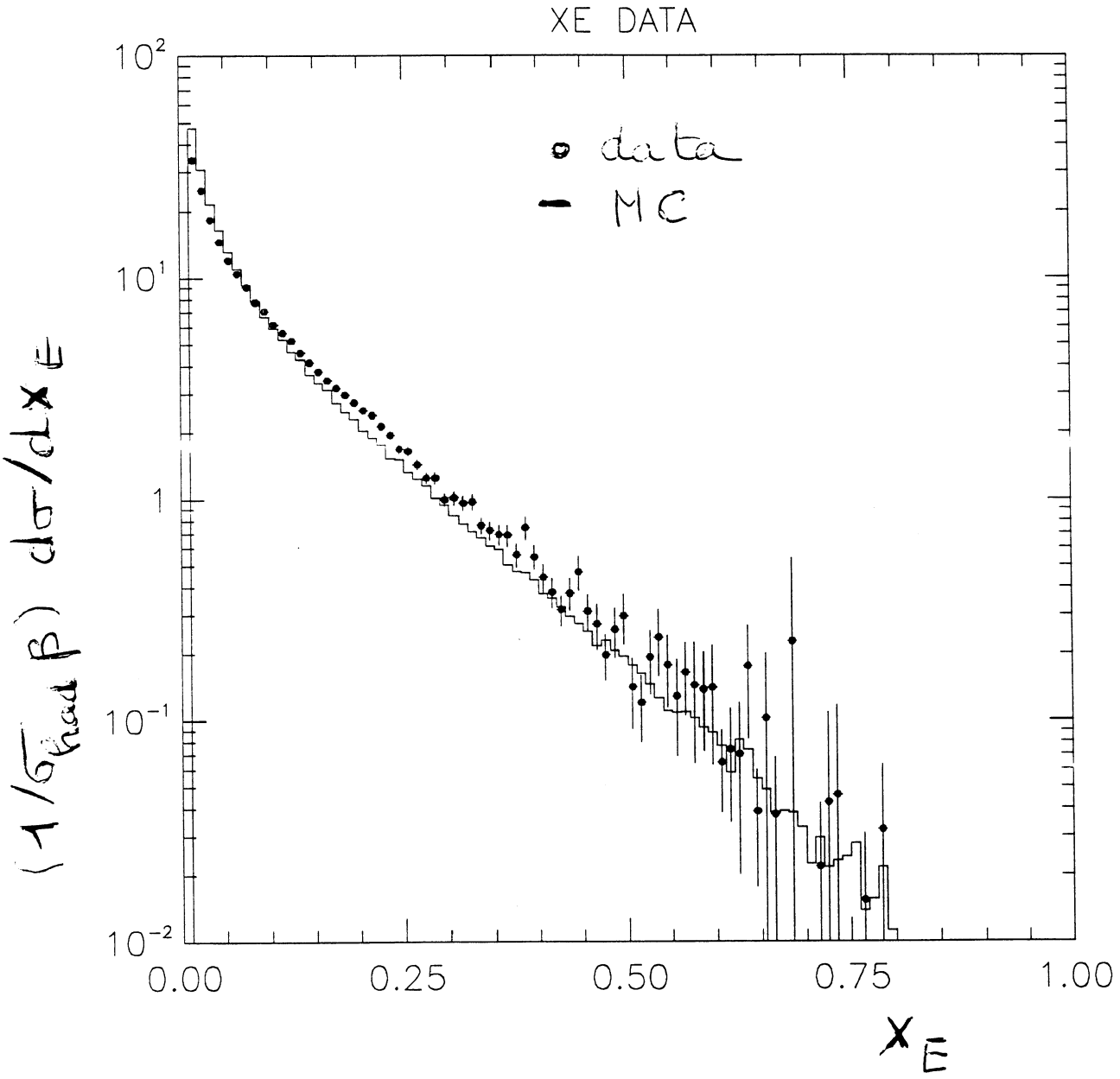

Fig. 7

File: Generated internally

ID	IDB	Symb	Date/Time	Area	Mean	R.M.S.
1443	40	-41	921118/1408	9.560	2.705	1.028
2014	40	1	921118/1606	10.17	2.906	1.069

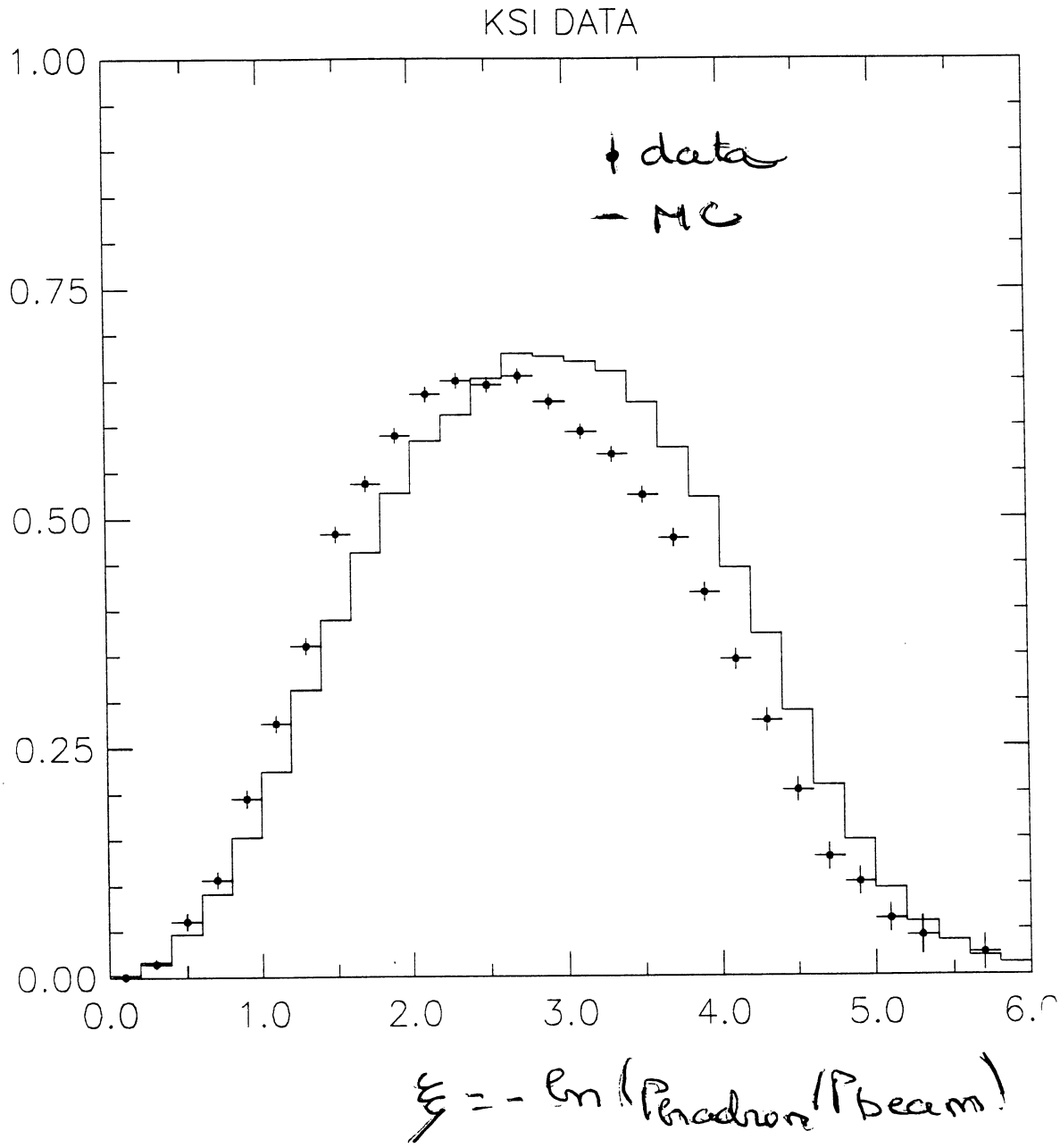

File: [LEMAIRE]XPEFFI.DAT;1

ID	IDB	Symb	Date/Time	Area	Mean	R.M.S.
1	10	1	000000/0000	9.778	0.2787	0.2134
1	20	2	000000/0000	2.003	0.1297	7.7674E-02

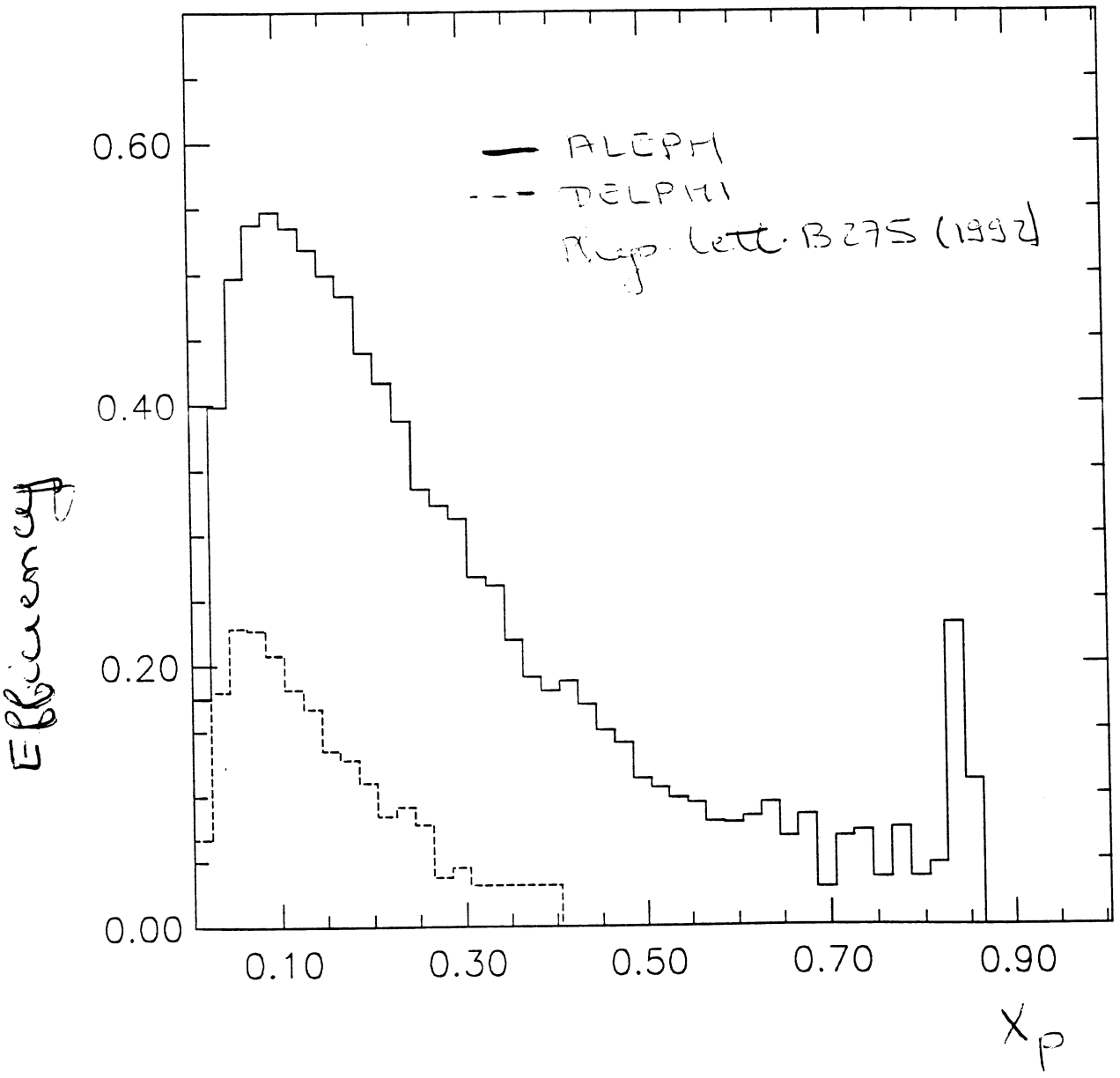

Fig 9

File: Generated internally

D	IDB	Symb	Date/Time	Area	Mean	R.M.S.
1	10	1	920910/1226	7.828	10.50	7.106

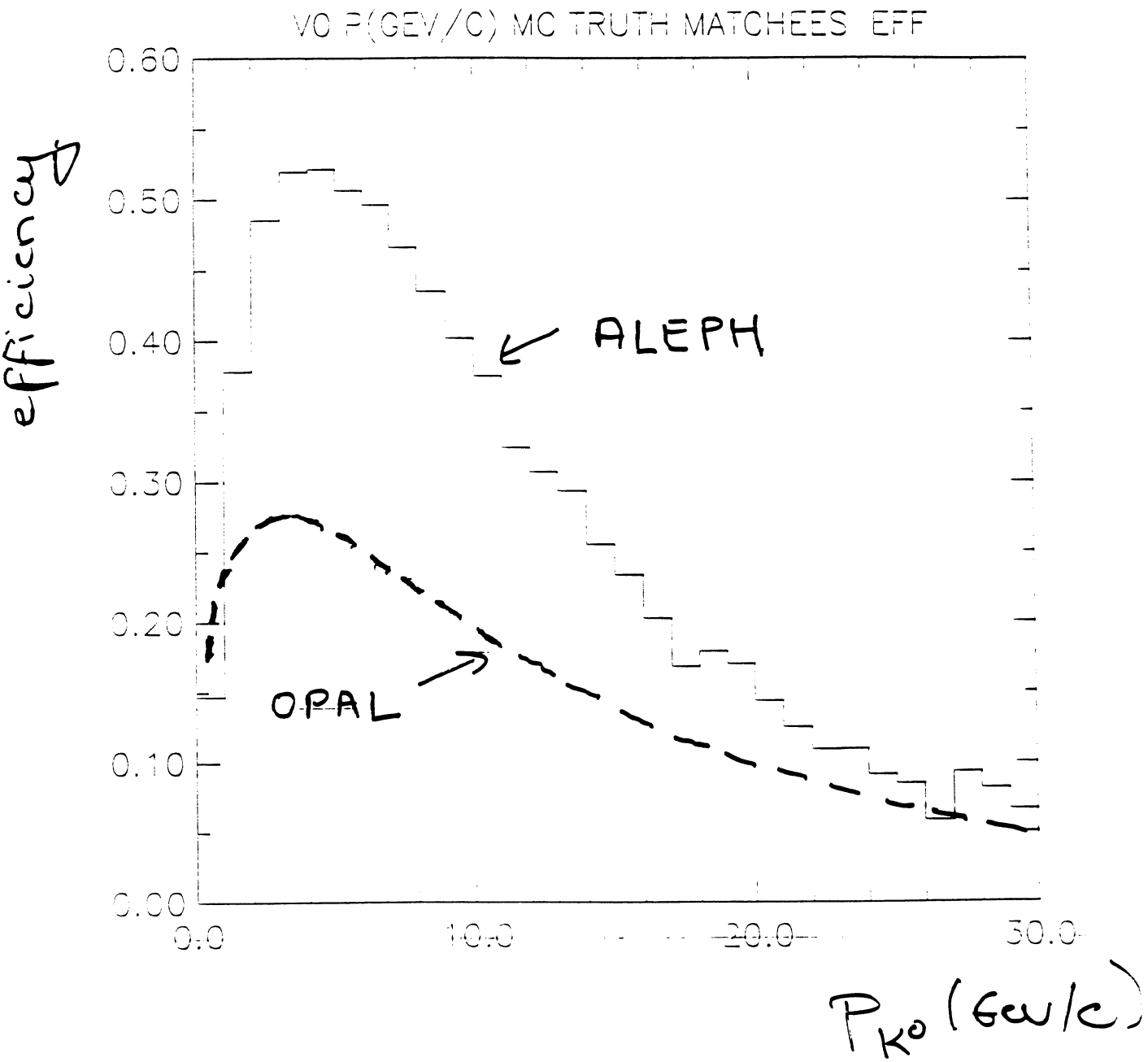

File: [LEMAIRE]XPDIST.DAT;1

ID	IDB	Symb	Date/Time	Area	Mean	R.M.S.
1444	30	-41	000000/0000	96.31	0.1079	0.1108
1444	40	41	000000/0000	99.10	8.7392E-02	7.3718E-02

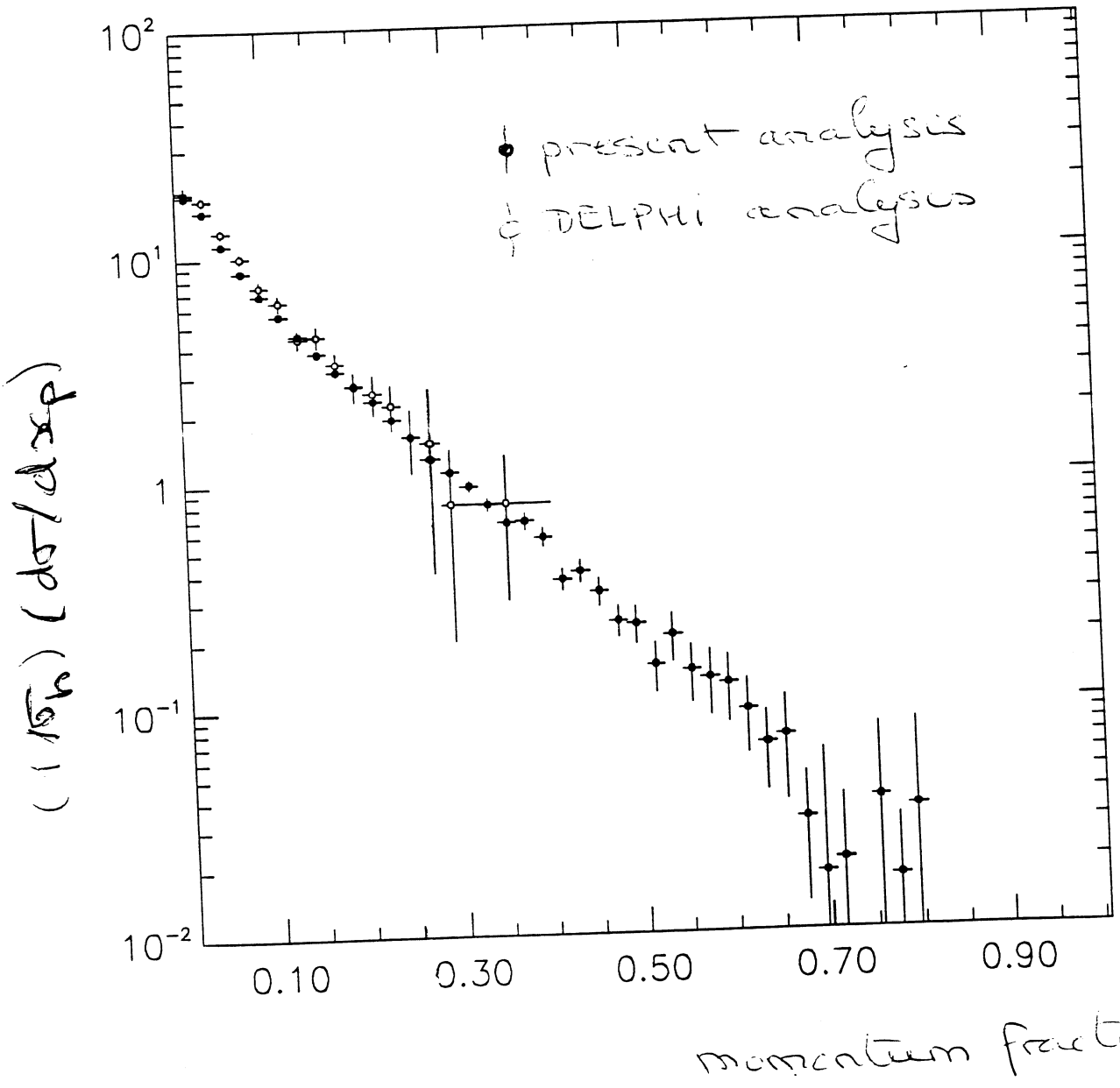

fig. 11

File: Generated internally

ID	IDB	Symb	Date/Time	Area	Mean	R.M.S.
1443	30	-41	921126/1043	9.609	2.701	1.028
1443	60	42	000000/0000	9.306	2.866	0.9086

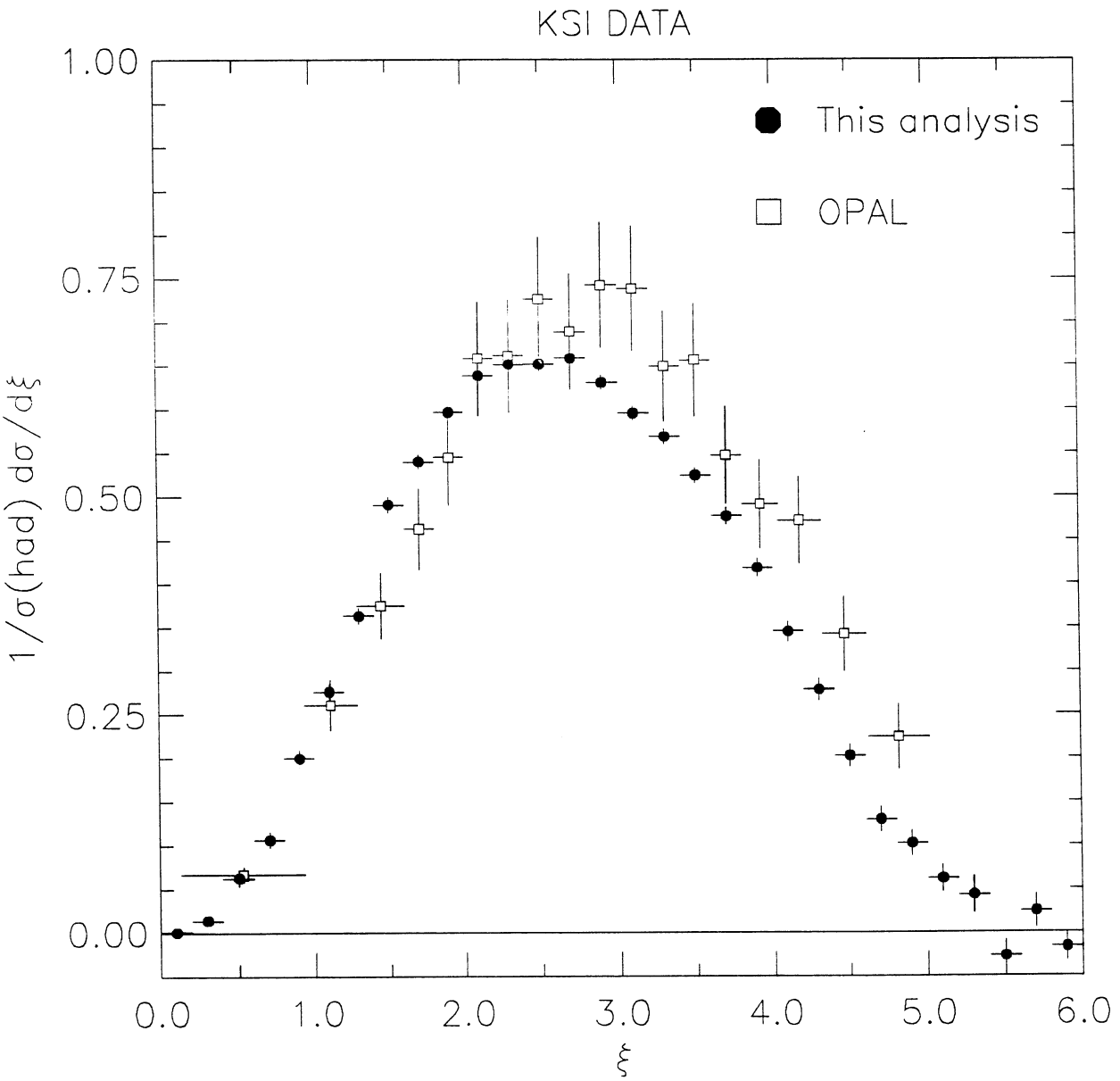

Fig. 12

File: [LEMAIRE]XKSIDIST.DAT;1

ID	IDB	Symb	Date/Time	Area	Mean	R.M.S.
1443	40	-41	000000/0000	9.560	2.705	1.028
1443	50	41	000000/0000	8.952	2.718	0.9064

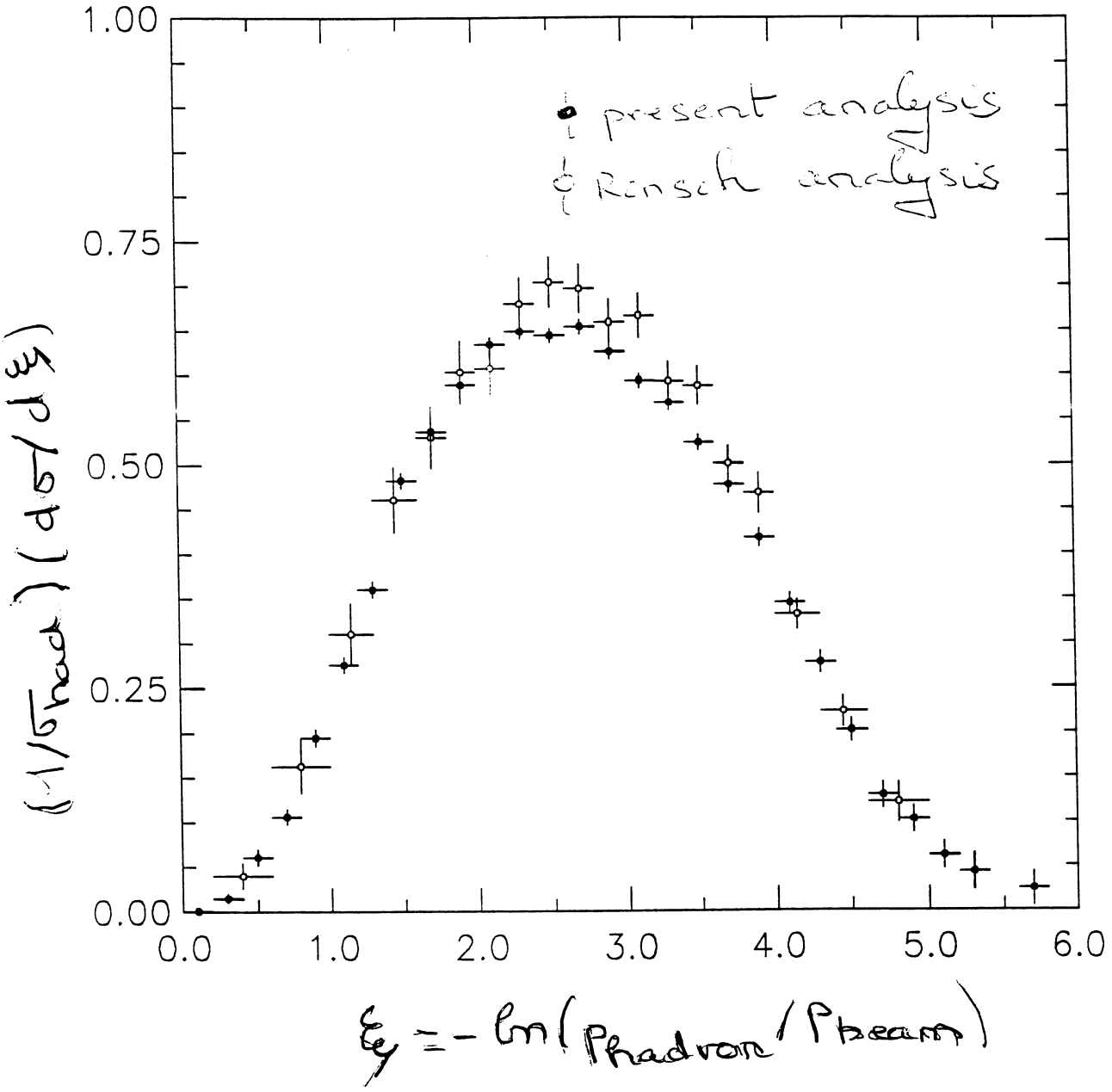

Fig: 13

File: [LEMAIRE]XKSIINT.DAT;2

ID	IDB	Symb	Date/Time	Area	Mean	R.M.S.
1443	50	-41	000000/0000	7.303	4.449	1.288
1443	60	41	000000/0000	9.628	3.166	1.243

$$\int_0^{\xi^{max}} \frac{dN}{d\xi}\, d\xi$$

$$\int_{x_p^{min}}^{1} \frac{dN}{dx_p}\, dx_p$$

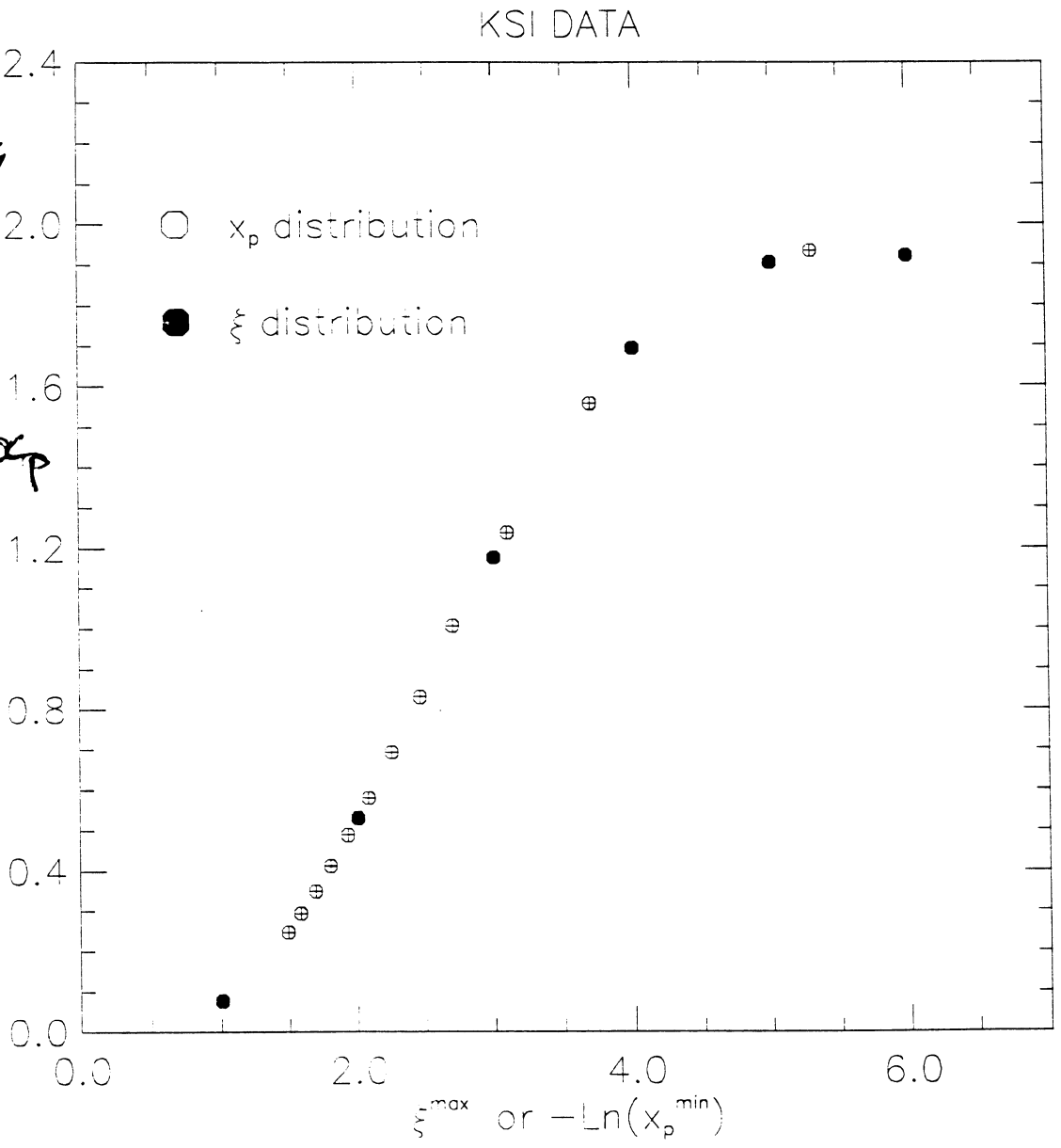

Fig. 14

File: Generated internally

ID	IDB	Symb	Date/Time	Area	Mean	R.M.S.
1460	20	-41	930118/1031	1.1516E+05	5.782	4.487
1460	22	1	930118/1034	1.1516E+05	5.423	4.304

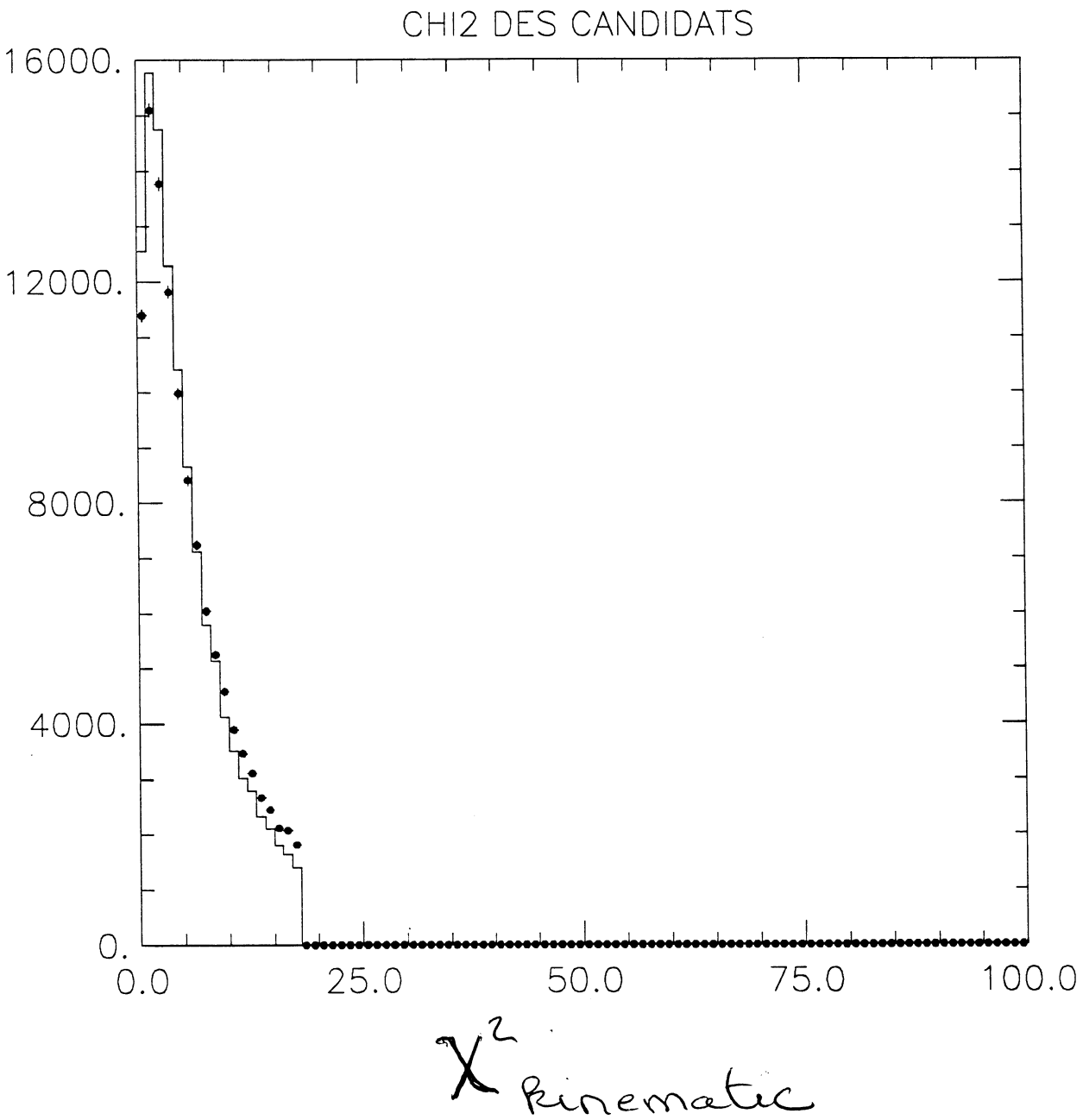

Fig. 15

File: [000000.LEMAIRE.KOSIDS5DT.HIS;1

ID	IDB	Symb	Date/Time	Area	Mean	R.M.S.
1461	0	-41	930118/1100	2.4377E+05	15.96	4.597
1461	11	1	930118/1235	2.4776E+05	16.27	4.687

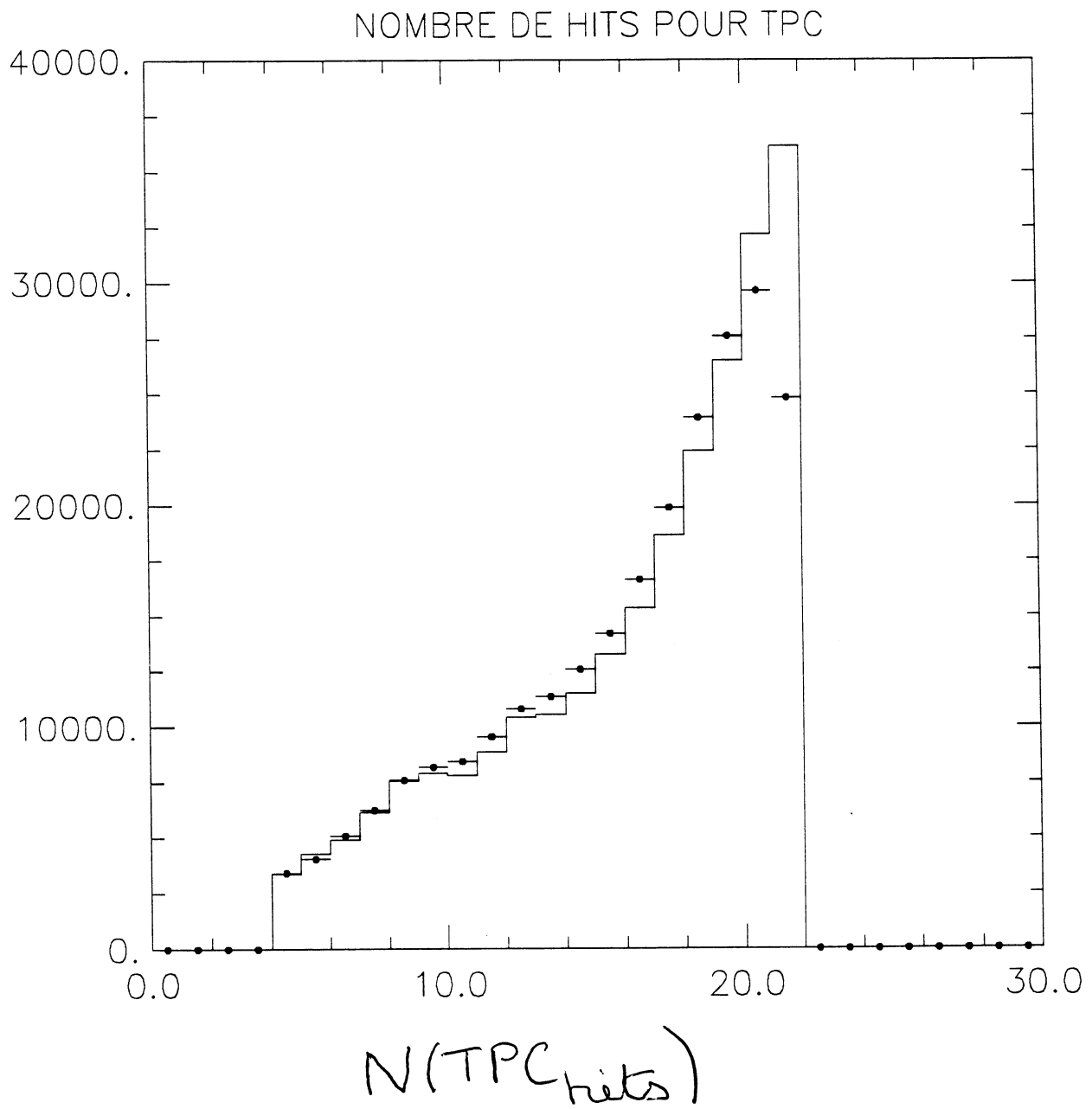

Fig. 16

MINUIT χ^2 Fit to Plot 1276&30
V0 (T/TAU) AFTER LAMBDA ELIM.
File: Generated internally
26-NOV-92 19:08:26
Plot Area Total/Fit 2.32932E+05 / 2.00864E+05
Func Area Total/Fit 3.00069E+05 / 1.99965E+05
χ^2= 87.4 for 92 - 2 d.o.f., C.L.= 55.7%

Errors		Parabolic	Minos	
Function 1: Exponential				
NORM	15200.	=83.04	-89.47	+90.99
SLOPE	1.0065	=1.7541E-03	-5.8584E-03	+5.8316E-03
★OFFSET	0.00000E+00	=0.0000E+00	-0.0000E+00	+0.0000E+00

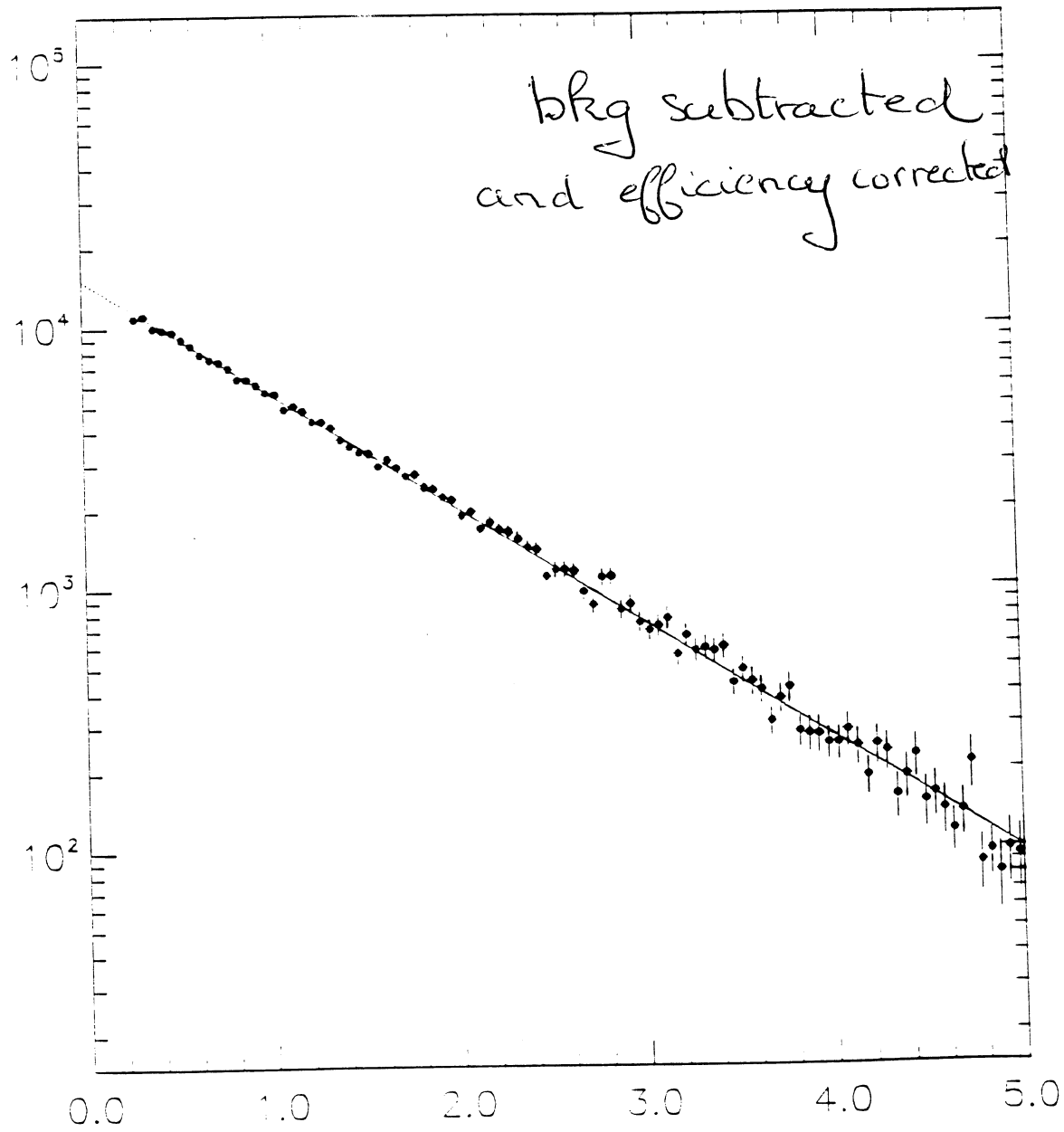

fig. 17